Constructing velocity-dependent potentials for screened Coulomb modified non-local interactions

D. Naik, B. Swain*, and U. Laha

[a] *Department of Physics, National Institute of Technology, Jamshedpur, Jharkhand, 831014, India,*
**e-mail:biswanathswain73@gmail.com*

Received 28 October 2024; accepted 11 November 2025

Energy-momentum-dependent potentials corresponding to a separable non-local potential and a local potential are created to explore nucleon-nucleon and nucleon-nucleus systems. There is either no hardcore or a quasi-hardcore in the created local potentials. Using the phase function method, elastic scattering phase shifts are calculated for the nucleon-nucleon and alpha-nucleon systems, yielding results that show reasonable agreement with experimental data. Utilising the s-wave phase parameters, the scattering cross sections are also estimated.

Keywords: Taylor series expansion; screened Coulomb plus non-local potential; energy-momentum dependent potential; phase parameters; cross sections.

DOI: https://doi.org/10.31349/RevMexFis.72.031201

1. Introduction

A comprehensive understanding of microscopic physical phenomena relies fundamentally on the quantum theory of scattering, which provides essential experimental insights into nucleon-nucleon (N-N) and nucleon-nucleus (N-A) interactions. Bound-state characteristics complement these observations, providing valuable insights into the nature of the underlying nuclear forces. At high energies, however, the conventional potential theory becomes inadequate, as static formulations fail to incorporate relativistic corrections and multiparticle production processes. The short-range component of the nuclear interaction arises primarily from multiple pion exchanges, where nucleon recoil effects cannot be neglected. Under such conditions, the N-N potential cannot be expressed solely in terms of the relative separation between two interacting particles. Instead, it must depend on the spatial coordinates of both nucleons, necessitating a nonlocal potential $V(r, r')$, that reflects the correlation between r and r'. The familiar local form $V(r)$ $\delta(r - r')$ thus represents a limiting case of this more general nonlocal description. Separable nonlocal interactions have been widely employed to describe various angular momentum states in both N-N and N-A scattering. Within optical model analyses, such nonlocal interactions are often approximated by equivalent energy-dependent local potentials, allowing direct comparison between the characteristics of nonlocal formulations and the phenomenology of local models. Numerous parametrisations of local potentials have been proposed in the literature to reproduce observed scattering data across different energy regimes. Building upon these approaches, the present work develops a phase-equivalent, velocity-dependent local potential that reproduces the behavior of screened, electromagnetic-modified nonlocal interactions within a simplified mathematical framework restricted to s-wave scattering. The analysis disregards spin dependence for simplicity. Earlier studies [1–10] have introduced several techniques for constructing phase-equivalent local potentials from separable nonlocal forms, with the supersymmetric (SUSY) formalism [11–16] offering a systematic approach to generate equivalent potentials while preserving the phase shifts of the parent interaction. Talukdar *et al*. [9] and Behera *et al*. [17] previously employed a Taylor expansion of the nonlocal wave function to establish equivalence with the Yamaguchi potential [18]. The pure Yamaguchi potential, being attractive, effectively reproduces low-energy phase parameters up to approximately 30 MeV but becomes inadequate at higher energies. To overcome this limitation, the proposed velocity-dependent local potential extends phase-shift calculations to a broader energy range while maintaining consistency with nonlocal scattering behaviour. The subsequent sections outline the localisation methodology and present the resulting phase-shift analyses, followed by concluding remarks.

2. Methodology

Non-local potentials are employed for various theoretical and practical reasons, either as independent models or in conjunction with local interactions. (a) Separable non-local potentials provide substantial mathematical simplification, as they often enable closed-form expressions for quantities such as wavefunctions, thereby making scattering problems more tractable. (b) The nucleon-nucleon (N-N) interaction in the $^1S_0$ and $^3S_1$ channels exhibits approximately separable t-matrix elements near zero energy; thus, separable models provide accurate approximations in this regime and, by construction, preserve unitarity. (c) Since the short-range N-N force is inherently non-local, adopting a separable representation constitutes an effective means of modelling this nonlocality. However, it is still valuable to construct local equivalent potentials, as they offer a clear physical interpretation

and allow one to determine whether the localized form of the interaction inevitably acquires momentum dependence. This is especially important when electromagnetic interactions are included alongside non-local nuclear forces, where momentum dependence may play a significant role. In the following, we demonstrate that a scattering problem formulated with a non-local potential can be reformulated in terms of an energy- and momentum-dependent local potential that reproduces the entire wavefunction of the original non-local interaction, not merely its asymptotic behaviour.

The rank-one Yamaguchi potential [18], a non-local interaction with a symmetric form factor, is defined as follows:

$$V(r,r') = \lambda g(r) g(r') = \lambda e^{-\beta r'} e^{-\beta r}, \tag{1}$$

where r denotes the separation between the interacting particles, λ is the strength parameter, and β is the inverse-range parameter. The Schrödinger equation for a system with a total interaction consisting of a local electromagnetic potential and a non-local nuclear potential takes the form of an integro-differential equation and is written as

$$\left[\frac{d^2}{dr^2} + \kappa^2 - V_a(r)\right] u_{ay}(\kappa, r) = \int_0^\infty V(r,r') u_{ay}(\kappa, r') dr'. \tag{2}$$

Here, $\kappa^2 = 2mE/\hbar^2$ and $V_a(r)$ denotes the atomic (electromagnetic) potential. In the present work, we consider three screened Coulomb-type electromagnetic potentials: the Manning-Rosen potential [19, 20], the Hellmann potential [21], and the Deng-Fan potential [22]. By applying a Taylor series expansion, the wave function $u_{ay}(\kappa, r)$ for the equivalent local potential is expressed as

$$u_{ay}(\kappa, r') = \sum_{n=0}^{\infty} \frac{(r'-r)^n}{n!} \frac{d^n}{dr^n} u_{ay}(\kappa, r). \tag{3}$$

Using Eq. (1) and Eq. (3) we write Eq. (2) as follows

$$\left[\frac{d^2}{dr^2} + \kappa^2 - V_a(r)\right] u_{ay}(\kappa, r) = \lambda e^{-\beta r} \times \sum_{n=0}^{\infty} \int_0^\infty \frac{(r'-r)^n}{n!} e^{-\beta r'} \frac{d^n}{dr^n} u_{ay}(\kappa, r) dr'. \tag{4}$$

Now expanding the terms in the RHS of Eq. (4) up to 2nd order (*i.e.* n=2) we obtain

$$\left[\frac{d^2}{dr^2} + \kappa^2 - V_a(r)\right] u_{ay}(\kappa, r) = \left[G_0(r) + G_1(r)\frac{d}{dr} + G_2(r)\frac{d^2}{dr^2}\right] u_{ay}(\kappa, r), \tag{5}$$

where

$$G_0(r) = \lambda e^{-\beta r} \int_0^\infty e^{-\beta r'} dr', \tag{6}$$

$$G_1(r) = \lambda e^{-\beta r} \int_0^\infty e^{-\beta r'} (r'-r) dr', \tag{7}$$

$$G_2(r) = \lambda e^{-\beta r} \int_0^\infty e^{-\beta r'} \frac{(r'-r)^2}{2} dr'. \tag{8}$$

On solving the integration, one gets

$$G_0(r) = \frac{\lambda}{\beta} e^{-\beta r}, \tag{9}$$

$$G_1(r) = \frac{\lambda}{\beta^2}\Big[1 - r\beta\Big] e^{-\beta r}, \tag{10}$$

and

$$G_2(r) = \frac{\lambda}{2\beta^3}\Big[1 + (1-r\beta)^2\Big] e^{-\beta r}. \tag{11}$$

On further simplification of Eq. (5) we get

$$\left[\frac{d^2}{dr^2} + \kappa^2 - \frac{V_a(r)}{1-G_2(r)}\right] u_{ay}(\kappa, r) = \left[V_A(\kappa, r) + V_B(r)\frac{d}{dr}\right] u_{ay}(\kappa, r), \tag{12}$$

where

$$V_A(\kappa, r) = \frac{G_0(r) - \kappa^2 G_2(r)}{1 - G_2(r)}, \tag{13}$$

$$V_B(r) = \frac{G_1(r)}{1 - G_2(r)}. \tag{14}$$

Expressing

$$V_{ay}(\kappa, r) = V_1(\kappa, r) + V_2(r)\frac{d}{dr}, \tag{15}$$

Eq. (12) is rewritten as

$$\left[\frac{d^2}{dr^2} + \kappa^2\right] u_{ay}(\kappa, r) = V_{ay}(\kappa, r) u_{ay}(\kappa, r). \tag{16}$$

Here we define $V_1(\kappa, r)$ and $V_2(r)$ such that

$$V_1(\kappa, r) = V_A(\kappa, r) + \frac{V_a(r)}{1 - G_2(r)}, \tag{17}$$

$$V_2(r) = V_B(r). \tag{18}$$

Using the values of $G_0(r)$, $G_1(r)$ and $G_2(r)$

$$V_A(\kappa, r) = \frac{(-2\beta^2 + (2 + r\beta(-2 + r\beta))\kappa^2)\lambda}{-2e^{r\beta}\beta^3 + (2 + r\beta(-2 + r\beta))\lambda}, \tag{19}$$

$$V_2(r) = V_B(r) = -\frac{2\beta(-1 + r\beta)\lambda}{2e^{r\beta}\beta^3 - (2 + r\beta(-2 + r\beta))\lambda}. \tag{20}$$

The potential $V_1(\kappa, r)$ depends on the specific screened Coulomb potential adopted, whereas $V_2(r)$ is independent of this choice. Consequently, the expression for $V_2(r)$ remains unchanged, while $V_1(\kappa, r)$ varies according to the selected form of the electromagnetic potential, as given below.

CASE 1-
For the Manning-Rosen potential, defined as

$$V_M(r) = \frac{1}{a^2}\left[\frac{p(p-1)}{(1-e^{-\frac{r}{a}})^2}e^{\frac{-2r}{a}} - \frac{Ae^{\frac{-r}{a}}}{1-e^{-\frac{r}{a}}}\right]. \tag{21}$$

the application of Eq. (17) yields

$$V_1(\kappa,r) = \frac{\frac{A-Ae^{\frac{r}{a}}+(-1+p)p}{a^2(-1+e^{\frac{r}{a}})^2}}{1-\frac{e^{-r\beta}(2+r\beta(-2+r\beta))\lambda}{2\beta^3}} + \frac{\frac{e^{-r\beta}(2\beta^2-(2+r\beta(-2+r\beta))\kappa^2)\lambda}{2\beta^3}}{1-\frac{e^{-r\beta}(2+r\beta(-2+r\beta))\lambda}{2\beta^3}}. \tag{22}$$

where A and p are dimensionless parameters characterising the strength of the potential, and a is the screening (or range) parameter that determines the spatial extent of the interaction.
CASE 2-
For the Hellmann potential, defined as

$$V_{He}(r) = \frac{Be^{-\delta r}}{r} - \frac{q}{r}. \tag{23}$$

the use of Eq. (17) yields

$$V_1(\kappa,r) = \frac{e^{-\delta r}(-2Be^{r\beta}\beta^3)}{r(-2e^{r\beta}\beta^3+(2+r\beta(-2+r\beta))\lambda)} + \frac{2e^{r\beta}q\beta^3+r(-2\beta^2+(2+r\beta(-2+r\beta))\kappa^2)\lambda}{r(-2e^{r\beta}\beta^3+(2+r\beta(-2+r\beta))\lambda)}. \tag{24}$$

The first term represents a Yukawa-type (exponentially screened) interaction that decays rapidly with increasing r. The second term corresponds to the long-range Coulomb interaction. Here, q denotes the Coulomb strength, B is the strength of the screened potential, and δ is the screening parameter that governs the range of the Yukawa component.
CASE 3-
The Deng-Fan potential (sometimes referred to as the improved Manning-Rosen potential) is defined as.

$$V_D(r) = \frac{v_1e^{-\gamma r}}{(1-e^{-\gamma r})} + \frac{v_2e^{-2\gamma r}}{(1-e^{-\gamma r})^2}. \tag{25}$$

For this, Eq. (17) yields

$$V_1(\kappa,r) = \frac{2e^{r\beta}((-1+e^{r\gamma})v_1+v_2)\beta^3}{(-1+e^{r\gamma})^2(2e^{r\beta}\beta^3-(2+r\beta(-2+r\beta))\lambda)} - \frac{(-1+e^{r\gamma})^2(-2\beta^2+(2+r\beta(-2+r\beta))\kappa^2)\lambda}{(-1+e^{r\gamma})^2(2e^{r\beta}\beta^3-(2+r\beta(-2+r\beta))\lambda)}. \tag{26}$$

Here the dimensionless strength parameters are v_1 and v_2 and γ represents the inverse range screening parameter.

Calogero's classical phase-function technique [23] is not directly applicable in the present context, as it does not account for velocity-dependent interactions. To address this, the method requires modification for systems involving a velocity-dependent potential. Such an extension was first introduced by McKellar and May, and later further developed by Behera *et al.* [17, 24]. Employing this modified approach, the phase equation corresponding to Eq. (12) for the s-wave can be expressed as follows:

$$\delta'(\kappa,r) = -\kappa^{-1}\Big[(V_1(\kappa,r))\sin(\kappa r+\delta(\kappa,r)) + \kappa V_2(r)\cos(\kappa r+\delta(\kappa,r))\Big]\sin(\kappa r+\delta(\kappa,r)). \tag{27}$$

Integrating this equation from the origin to a sufficiently large radial distance within the asymptotic region using the fourth-order Runge-Kutta (RK4) method, and imposing the initial condition $\delta(\kappa,0)=0$, yields the scattering phase function $\delta(\kappa,r)$. The scattering phase shift is then obtained as

$$\delta(\kappa) = \lim_{r\to\infty}\delta(\kappa,r).$$

Once the phase shift $\delta(\kappa)$ is determined, the total s-wave scattering cross-section can be calculated using the relation

$$\sigma_{\text{total}} = \frac{4\pi}{\kappa^2}\sin^2\delta(\kappa). \tag{28}$$

Since the s-wave has both triplet and singlet state contributions, its total cross-section is

$$\sigma_{\text{total}} = \frac{3}{4}\sigma_{\text{triplet}} + \frac{1}{4}\sigma_{\text{singlet}}. \tag{29}$$

The differential cross-section for all partial waves is

$$\sigma(\theta) = |f_a(\theta) + f_n(\theta)|^2, \quad (30)$$

where

$$f_a(\theta) = -\left[\frac{\eta}{2\kappa \sin^2(\theta/2)}\right] e^{-i\eta \ln \sin^2(\theta/2) + 2i\sigma(\eta)}, \quad (31)$$

and

$$f_n(\theta) = \frac{1}{2i\kappa} \sum_{l=0}^{\infty} (2l+1) e^{2i\sigma_l(\eta)} P_l(\cos\theta)(S_l - 1), \quad (32)$$

with

$$S_l = e^{2i\delta_l}. \quad (33)$$

3. Results and discussion

The best-fit parameters associated with different local potentials are listed in tabular form (Tables I to III) along with those of the non-local potential. Using these values, we have plotted velocity-dependent and independent potentials for a certain range of r. Also, we have calculated the scattering phase shift using Eq. (27). Then, we calculated the total cross-section associated with neutron-proton, proton-proton, and alpha-neutron systems, as well as the differential cross-section for the alpha-proton system. For the computation we have used the value $\hbar^2/2m = 41.47$ MeV fm^2 for the nucleon-nucleon system and $\hbar^2/2m = 25.92$ MeV fm^2 for alpha-nucleon system.

The potential graphs for the various states of the n-n and α-n systems are shown in Figs. 1a)-1c). Since both systems are charge-independent, the choice of electromagnetic potential does not affect the results. For a given set of parameters for the nuclear potential, the curves corresponding to identical states in these systems remain unchanged.

Similarly, Figs. 1d)-1i) present the potential graphs for the p-p and α-p systems. From these plots, it is observed that the depth of the potentials decreases with increasing kinetic energy of the projectile, which is consistent with the findings reported in Refs. [25,26]. An increase in potential energy below a certain value of r indicates the presence of a repulsive core, which becomes more clearly visible at higher energies. The appearance of quasi-hard-core potentials at higher energies suggests that our energy-dependent nucleon-nucleon and α-nucleon potentials are in good agreement with standard nuclear potential models.

In the p-p and α-p systems, the projectile experiences not only nuclear repulsion but also electromagnetic repulsive forces. Overall, the results indicate that our energy-dependent potentials exhibit a diffuse hard core at very short

TABLE I. Parameters for Manning-Rosen Potential plus Yamaguchi potential.

System	State	λ(fm^{-3})	β(fm^{-1})	a(fm)	A	p
p-p	$^1S_0$	-7.45	1.601	20.804	-0.42	-0.001
n-p	$^1S_0$	-7.45	1.601	20.804	0	0
	$^3S_1$	-17.201	1.909	20.804	0	0
α-p	$(1/2)^+$	-36.100	1.41	30.140	-2.199	-0.001
α-n	$(1/2)^+$	-11.27	1.4	19.940	0	0

TABLE II. Parameters for Hellmann Potential plus Yamaguchi potential.

System	State	λ(fm^{-3})	β(fm^{-1})	δ(fm^{-1})	B(fm^{-1})	q(fm^{-1})
p-p	$^1S_0$	-7.45	1.601	20.804	-0.42	-0.001
n-p	$^1S_0$	-7.45	1.601	0.05	0	0
	$^3S_1$	-17.201	1.909	0.05	0	0
α-p	$(1/2)^+$	-36.100	1.41	0.046	0.025	-0.054
α-n	$(1/2)^+$	-11.27	1.4	19.940	0	0

TABLE III. Parameters for Deng-Fan Potential plus Yamaguchi potential.

System	State	λ(fm^{-3})	β(fm^{-1})	γ(fm^{-1})	v_1(fm^{-2})	v_2(fm^{-2})
p-p	$^1S_0$	-7.45	1.601	0.60	0.025	-0.001
n-p	$^1S_0$	-7.45	1.601	0.60	0	0
	$^3S_1$	-17.201	1.909	0.60	0	0
α-p	$(1/2)^+$	-36.100	1.41	0.70	0.239	-0.001
α-n	$(1/2)^+$	-11.27	1.4	19.940	0	0

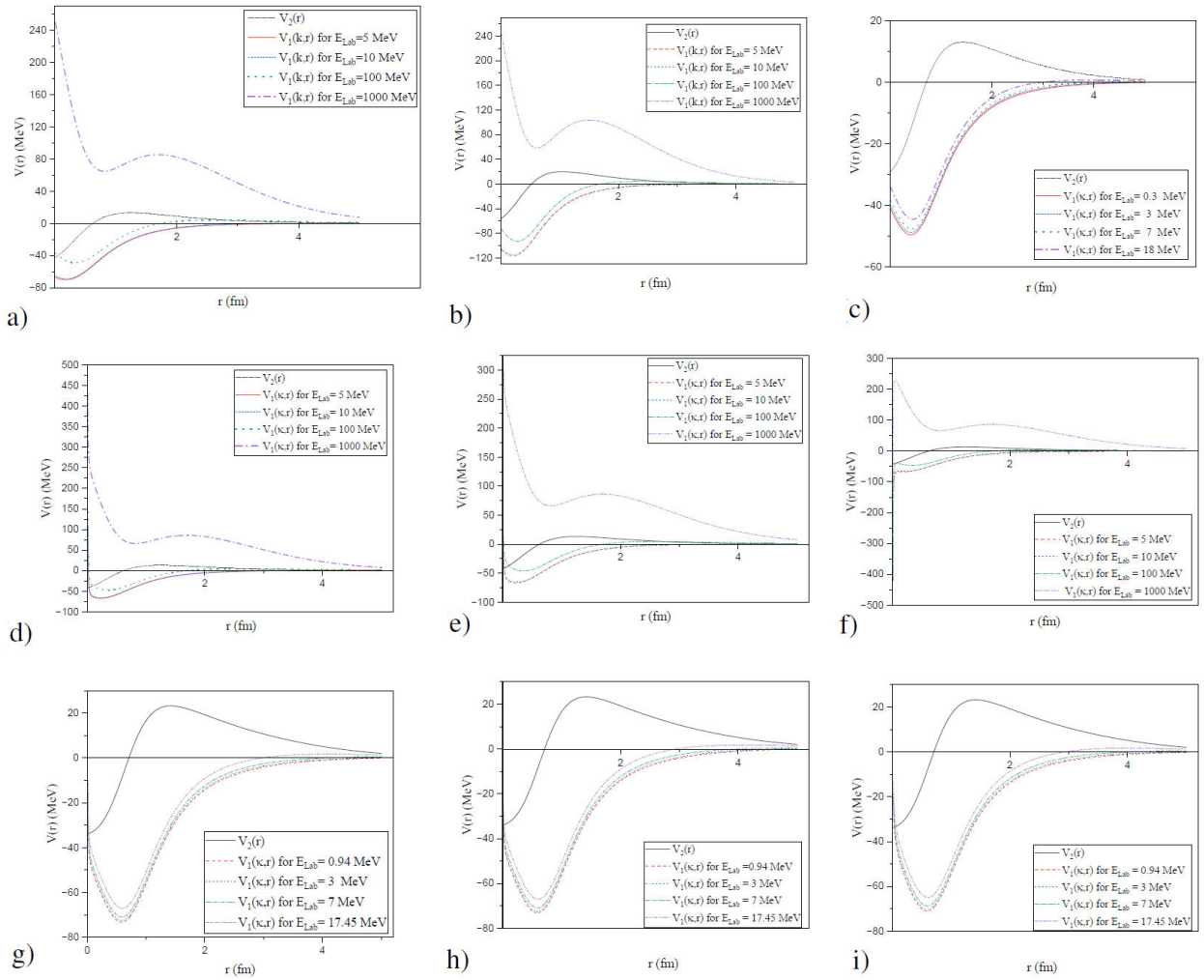

FIGURE 1. Potential plots as a function of r. a) n-p $^1S_0$, b) n-p $^3S_1$, c) α-n, d) Manning–Rosen p-p $^1S_0$, e) Hellmann p-p $^1S_0$, f) Deng-Fan p-p $^1S_0$, g) Manning-Rosen $\alpha - p$, h) Hellmann α-p, i) Deng-Fan α-p.

distances. Furthermore, the potential for the α-p system shows a stronger short-range repulsion compared to the α-n system.

We have also determined the scattering phase shifts for these systems. The phase parameters for the n-p $^1S_0$ state are shown in Fig. 2. These results are identical for all the potentials considered and are in agreement with the findings of Pérez *et al.* [27] and Arndt *et al.* [28]. It is observed that our results are consistent with those of Ref. [27] up to $E_{Lab} = 350$ MeV, with a maximum deviation of 2.96° from Ref. [28]. The phase shift for this state changes sign at approximately $E_{Lab} = 266$ MeV. The phase shift for the n-p $^3S_1$ state, presented in Fig. 3, shows good agreement with both Pérez *et al.* [27] and Arndt *et al.* [28] up to $E_{Lab} = 350$ MeV. Beyond this energy, the results begin to diverge, with a maximum difference of 18.33° at $E_{Lab} = 1050$ MeV compared to Arndt *et al.* [28]. This discrepancy may be attributed to the omission of additional interactions, such as spin-spin and tensor interactions, from our potential model. For this state, the phase shift changes sign at around $E_{\rm Lab} = 350$ MeV. The phase shift for the α-n system, shown in Fig. 4, exhibits

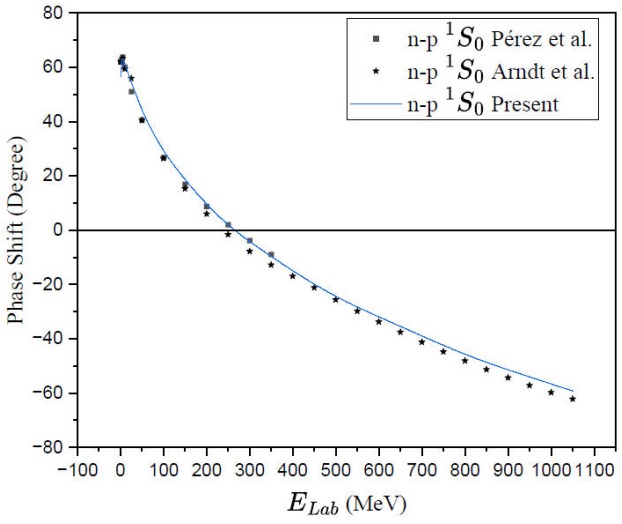

FIGURE 2. n-p $^1S_0$ scattering phase shift as a function of $E_{\rm Lab}$. Standard data are from Ref. [27,28].

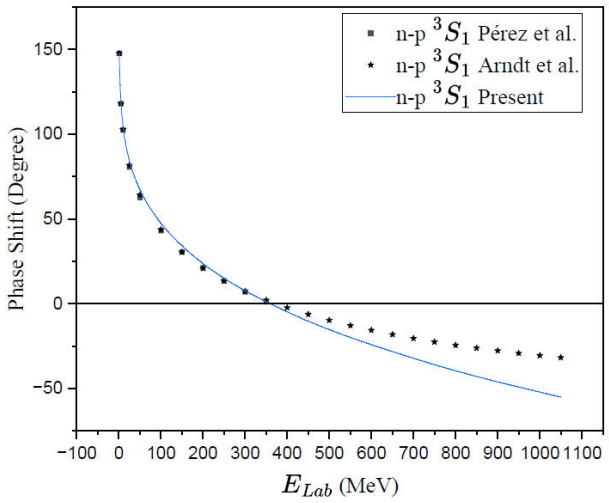

FIGURE 3. n-p $^3S_1$ scattering phase shift as a function of E_{Lab}. Standard data are from Ref. [27,28].

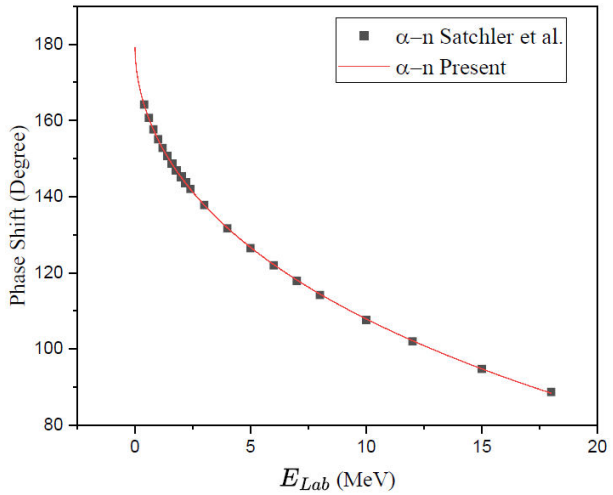

FIGURE 4. α-n scattering phase shift as a function of E_{Lab}. Standard data are from Ref. [29].

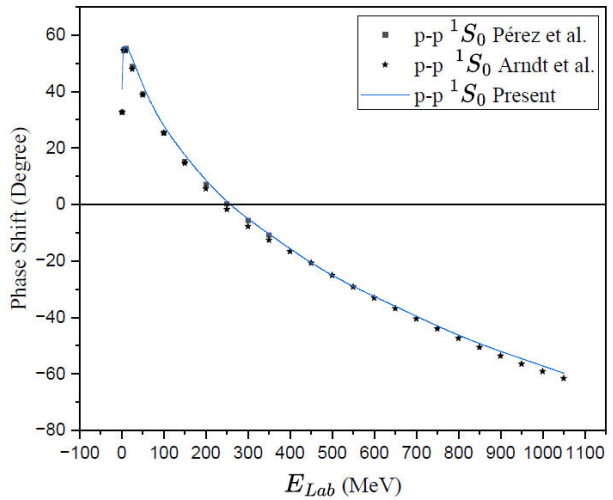

FIGURE 5. Manning-Rosen p-p $^1S_0$ scattering phase shift as a function of E_{Lab}. Standard data are from Ref. [27,28].

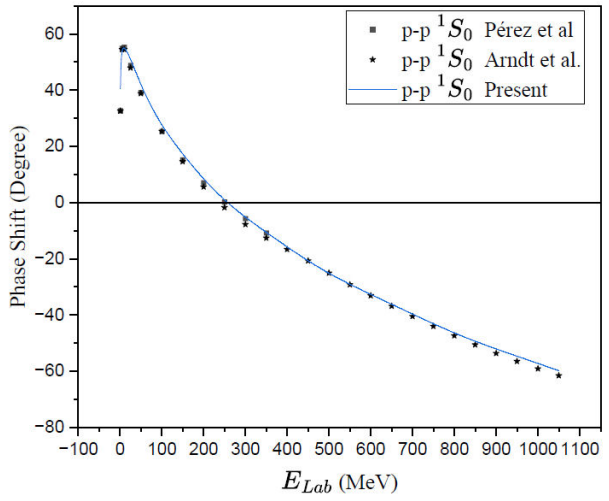

FIGURE 6. Deng-Fan p-p $^1S_0$ scattering phase shift as a function of E_{Lab}. Standard data are from Ref. [27,28].

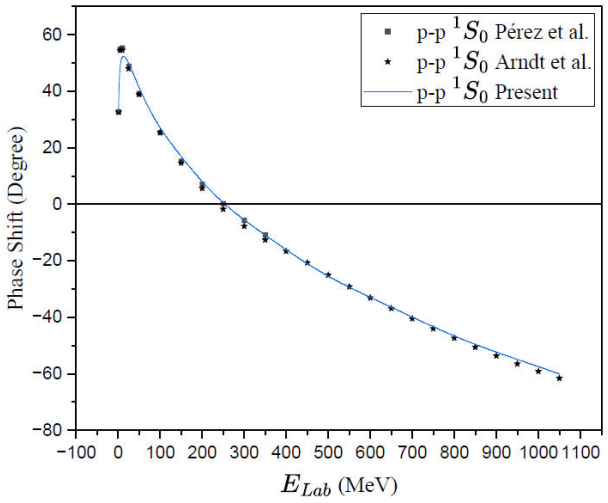

FIGURE 7. Hellmann p-p $^1S_0$ scattering phase shift as a function of E_{Lab}. Standard data are from Ref. [27,28].

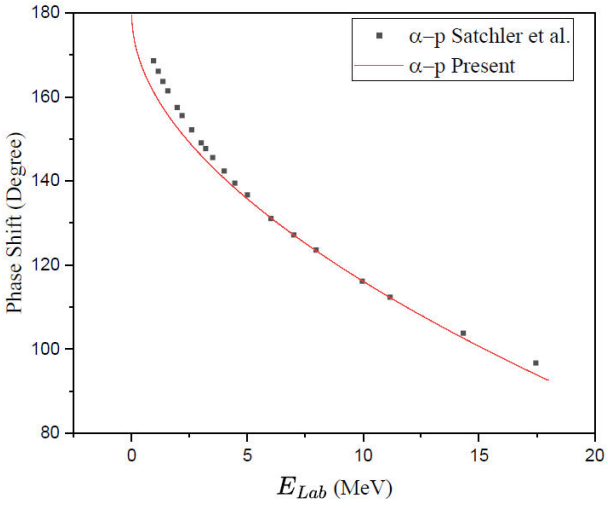

FIGURE 8. Hellmann α-p scattering phase shift as a function of E_{Lab}. Standard data are from Ref. [29].

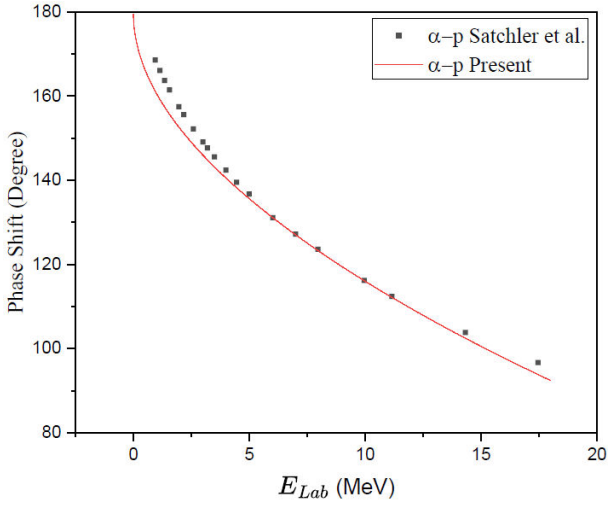

FIGURE 9. Manning-Rosen α-p scattering phase shift as a function of E_{Lab}. Standard data are from Ref. [29].

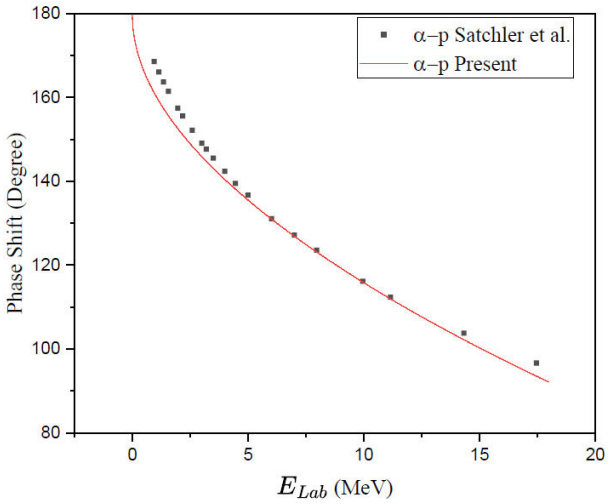

FIGURE 10. Deng-Fan α-p scattering phase shift as a function of E_{Lab}. Standard data are from Ref. [29].

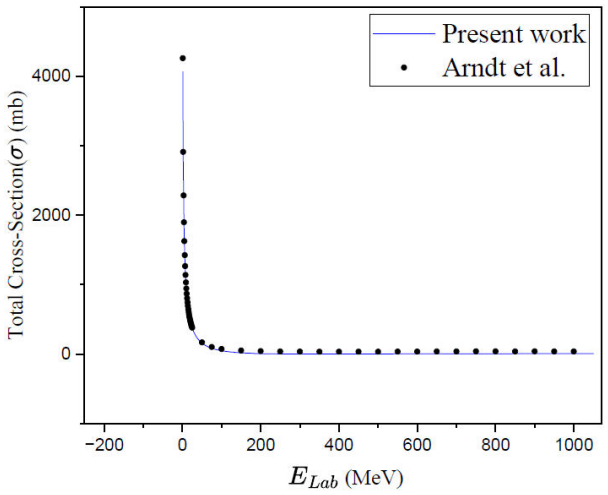

FIGURE 11. n-p total cross-section as a function of E_{Lab}. Standard data are from Ref. [30].

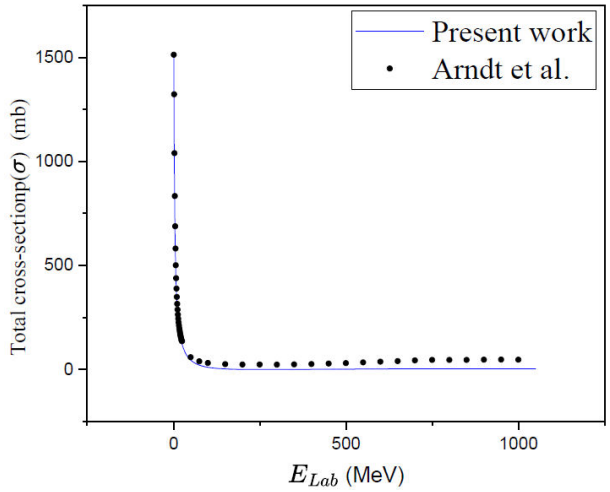

FIGURE 12. p-p total cross-section as a function of E_{Lab}. Standard data are from Ref. [30].

good agreement with the results of Satchler *et al.* [29]. We observe that the scattering phase shifts for this system remain unchanged regardless of the choice of electromagnetic potential.

Figures 5-7 illustrate the phase shifts for the p-p system. For the Manning-Rosen potential, the results are in good agreement with those of Pérez *et al.* [27] and Arndt *et al.* [28], except at $E_{Lab} = 1$ MeV. A similar trend is observed for the Deng-Fan potential. In contrast, the phase shifts obtained using the Hellmann potential show good agreement with the reference data except in the vicinity of the peak value. We obtain a peak at $E_{Lab} = 13$ MeV with a phase shift of 52.37°, which is slightly lower than the standard data reported by Arndt *et al.* [28].

Figures 8, 9, and 10 present the phase shifts for the α-p system. The results for all three potentials show reasonable agreement with those of Satchler *et al.* [29], with only a slight deviation observed below $E_{Lab} = 5$ MeV. This consistent trend is observed across all three velocity-dependent potentials.

Figures 11-13 present the total cross sections for the n-p, p-p, and α-n systems, calculated using Eqs. (28) and (29). For the n-p system, the total cross section follows the expected trend and shows good agreement with the data reported by Arndt *et al.* [30] up to an incident energy of approximately 25 MeV. Beyond this energy, noticeable deviations are observed. In particular, at 1000 MeV, the calculated total cross section is 6.69 mb, whereas the value reported in Ref. [30] is 38.14 mb. A similar discrepancy is observed for the p-p system, where the maximum deviation in the total cross section is 43.49 mb at around 1000 MeV.

For the α-n system, the calculated total cross sections do not reproduce the results of Haesner *et al.* [31], with substantial differences occurring especially at low energies. This discrepancy is expected, as contributions from higher partial

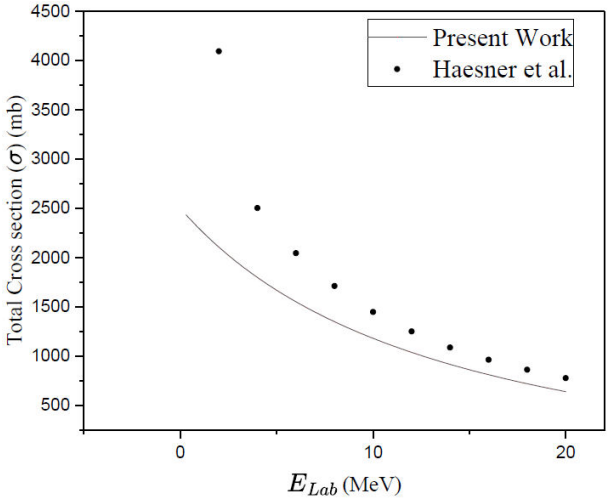

FIGURE 13. α-n total cross-section as a function of $E_{\rm Lab}$. Standard data are from Ref. [31].

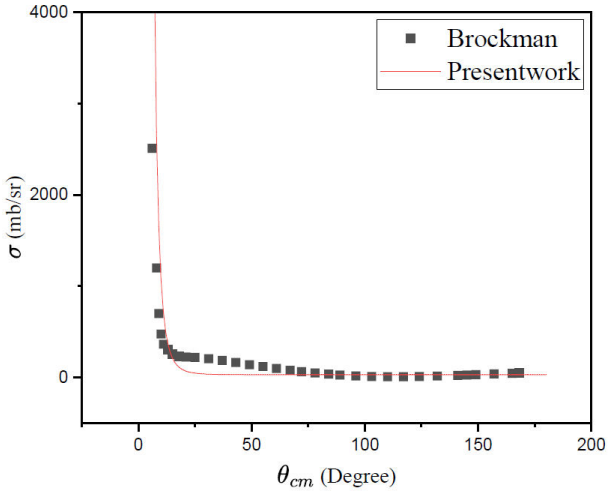

FIGURE 14. α-p differential cross-section at $E_{\rm Lab} = 17.45$ MeV. Standard data are from Ref. [32].

waves were not included in the present calculation. Nevertheless, based on the observed trend, it may be anticipated that improved agreement could be achieved at higher energies and with the inclusion of contributions from higher partial waves.

Figure 14 presents the differential cross section for the α-p system, calculated using Eq. (30). The results show reasonable agreement with those reported by Brockman [32] at forward and backward scattering angles; however, noticeable discrepancies are observed in the intermediate angular region. According to Ref. [32], the minimum value of the differential cross section occurs at approximately 110°, with a magnitude of 7.57 mb/sr. In contrast, no such minimum is observed in the present calculation. Instead, the differential cross section remains nearly constant for angles above 80°, with an average value of about 29.83 mb/sr. These discrepancies in the total and differential scattering cross sections for the nucleon-nucleon and α-nucleon systems may be attributed to the omission of higher partial-wave contributions in the present analysis.

4. Conclusion

Efforts to localise non-local nuclear potentials, or to construct phase-equivalent local representations of such interactions, have been undertaken by several research groups. In this work, we develop an energy-dependent local potential obtained by localising non-local interactions supplemented with screened Coulomb local contributions. By applying a Taylor series expansion of the wavefunctions, the corresponding phase parameters are obtained and subsequently used to compute elastic scattering cross sections. The resulting local potentials reproduce phase shifts in close agreement with standard benchmark data over an extended range of incident energies. Since folding models for α-nucleus scattering commonly employ non-local separable interactions or their phase-equivalent local forms, we have developed velocity-dependent interaction models for nucleon-nucleon and α-nucleon systems. The results demonstrate the effectiveness and applicability of the proposed framework, which can be further generalised to higher-rank and electromagnetically distorted non-local potentials. We demonstrate that a non-local, separable potential, considered independently or in combination with a local contribution, can be reformulated as an energy- and momentum-dependent local potential. Although the present results for the $^1S_0$ and $^3S_1$ channels exhibit certain limitations, the approach remains theoretically promising. The long-range part of the nucleon-nucleon interaction is well represented by the one-pion-exchange potential (OPEP). This is supported by the observation that the phase shifts for higher partial waves $\ell < 3$ are reproduced very well by OPEP alone within the energy range of 0-300 MeV. However, the situation for higher angular momentum states is less conclusive. Behera *et al.* [33] reported that the energy- and momentum-dependent local potential remains phase-equivalent up to the partial wave $\ell = 2$, whereas for higher partial waves the method does not yield satisfactory results. This discrepancy may be attributed to the high-momentum components of the non-local wavefunction $\ell > 2$, which differ significantly from those generated by the corresponding energy- and momentum-dependent local potential. The residual deviations at higher energies are attributed to the current exclusion of spin-spin interactions, which is being addressed. Future work will incorporate spin dependence and extend the framework to treat all partial waves within a unified theoretical formulation.

1. N. Levinson, Determination of the potential from the asymptotic phase, *Physical Review* **75** (1949) 1445, https://doi.org/10.1103/PhysRev.75.1445
2. V. Bargmann, Remarks on the determination of a central field of force from the elastic scattering phase shifts, *Physical Review* **75** (1949) 301, https://doi.org/10.1103/PhysRev.75.301
3. K. Chadan and P. C. Sabatier, Inverse problems in quantum scattering theory (Springer Science and Business Media, 2012).
4. P. Abraham and H. Moses, Changes in potentials due to changes in the point spectrum: anharmonic oscillators with exact solutions, *Physical Review A* **22** (1980) 1333, https://doi.org/10.1103/PhysRevA.22.1333
5. I. M. Gel'fand and B. M. Levitan, On the determination of a differential equation from its spectral function, *Izvestiya Rossiiskoi Akademii Nauk. Seriya Matematicheskaya* **15** (1951) 309.
6. M. Coz, L. G. Arnold, and A. D. MacKellar, Nonlocal potentials and their local equivalents, *Annals of Physics* **59** (1970) 219, https://doi.org/10.1016/0003-4916(70)90401-X
7. L. G. Arnold and A. D. MacKellar, Study of equivalent local potentials obtained from separable two-nucleon interactions, *Physical Review C* **3** (1971) 1095, https://doi.org/10.1103/PhysRevC.3.1095
8. J. McTavish, Separable potentials and their momentum-energy dependence, *Journal of Physics G: Nuclear Physics* **8** (1982) 1037, https://doi.org/10.1088/0305-4616/8/8/010
9. B. Talukdar, G. Sett, and S. Bhattaru, On the localisation of separable non-local potentials, *Journal of Physics G: Nuclear Physics* **11** (1985) 591, https://dx.doi.org/10.1088/0305-4616/11/5/006
10. A. Behera *et al*., Applicability of Phase-Equivalent Energy-Dependent Potential. Case Studies, *Physics of Atomic Nuclei* **85** (2022) 124, https://doi.org/10.1134/S1063778822010057
11. C. Sukumar, Supersymmetric quantum mechanics and the inverse scattering method, *Journal of Physics A: Mathematical and General* **18** (1985) 2937, https://dx.doi.org/10.1088/0305-4470/18/15/021
12. D. Pursey, Isometric operators, isospectral Hamiltonians, and supersymmetric quantum mechanics, *Physical Review D* **33** (1986) 2267, https://doi.org/10.1103/PhysRevD.33.2267
13. D. Baye, Supersymmetry between deep and shallow nucleusnucleus potentials, *Physical Review Letters* **58** (1987) 2738, https://doi.org/10.1103/PhysRevLett.58.2738
14. R. Amado, Phase-equivalent supersymmetric quantummechanical partners of the Coulomb potential, *Physical Review A* **37** (1988) 2277, https://doi.org/10.1103/PhysRevA.37.2277
15. A. Khare and U. Sukhatme, Phase-equivalent potentials obtained from supersymmetry, *Journal of Physics A: Mathematical and General* **22** (1989) 2847, https://dx.doi.org/10.1088/0305-4470/22/14/031
16. M. Majumder and U. Laha, Phase-equivalent potentials using SUSY transformations, *Pramana* **96** (2022) 145, https://doi.org/10.1007/s12043-022-02390-3
17. A. K. BEHERA, U. LAHA, and J. BHOI, Generating velocitydependent potential in all partial waves, *Turkish Journal of Physics* **44** (2020) 229, https://doi.org/10.3906/fiz-1909-16
18. Y. Yamaguchi, Two-nucleon problem when the potential is nonlocal but separable. I, *Physical Review* **95** (1954) 1628, https://doi.org/10.1103/PhysRev.95.1628
19. M. F. Manning and N. Rosen, A potential function for the vibrations of diatomic molecules, *Phys. Rev.* **44** (1933) 951
20. B. Khirali *et al*., Scattering with Manning-Rosen potential in all partial waves, *Annals of Physics* **412** (2020) 168044, https://doi.org/10.1016/j.aop.2019.168044
21. H. Hellmann, A combined approximation method for the energy calculation in the many-electron problem, Acta Physicochim. *URSS* **1** (1935) 913
22. Z. Deng and Y. Fan, A potential function of diatomic molecules. J. Shandong *Univ. Nat. Sci.* **1** (1957)
23. F. Calogero, Variable Phase Approach to Potential Scattering by F Calogero (Elsevier, 1967).
24. B. McKellar and R. May, Theory of low energy scattering by velocity dependent potentials, *Nuclear Physics* **65** (1965) 289, https://doi.org/10.1016/0029-5582(65)90269-5
25. L. G. Arnold and A. D. MacKellar, Study of equivalent local potentials obtained from separable two-nucleon interactions, *Physical Review C* **3** (1971) 1095, https://doi.org/10.1103/PhysRevC.3.1095
26. U. Laha, S. K. Das, and J. Bhoi, Localization of a nonlocal interaction, *Turkish Journal of Physics* **41** (2017) 447, https://doi.org/10.3906/fiz-1704-23
27. R. N. Pérez, J. Amaro, and E. R. Arriola, The low-energy structure of the nucleon-nucleon interaction: statistical versus systematic uncertainties, *Journal of Physics G: Nuclear and Particle Physics* **43** (2016) 114001
28. R. A. Arndt *et al*., Nucleon-nucleon partial-wave analysis to 1 GeV, *Physical Review D* **28** (1983) 97, https://doi.org/10.1103/PhysRevD.28.97
29. G. Satchler *et al*., An optical model for the scattering of nucleons from 4He at energies below 20 MeV, *Nuclear Physics A* **112** (1968) 1, https://doi.org/10.1016/0375-9474(68)90216-9
30. R. Arndt *et al*., Absolute Total np and pp Cross-Section Determinations, *Nuclear science and engineering* **162** (2009) 312, https://doi.org/10.13182/NSE162-312
31. B. Haesner *et al*., Measurement of the he 3 and he 4 total neutron cross sections up to 40 mev, *Physical Review C* **28** (1983) 995, https://doi.org/10.1103/PhysRevC.28.995
32. K. W. Brockman, Scattering of Protons by Helium between 11.4 Mev and 18 Mev, *Physical Review* **108** (1957) 1000, https://doi.org/10.1103/PhysRev.108.1000
33. A. Behera *et al.*, Applicability of phase-equivalent energydependent potential. case studies, *Physics of Atomic Nuclei* **85** (2022) 124, https://doi.org/10.1134/S1063778822010057